High excitation ISM and gas[*]

E. Peeters
NASA Ames Research Center, USA

N.L. Martín-Hernández
Observatoire de Geneve, Switzerland

N.J. Rodríguez-Fernández
LUTH / LERMA - Observatoire de Paris, France

A.G.G.M. Tielens
Kapteyn Astronomical Institute, The Netherlands

Abstract. An overview is given of ISO results on regions of high excitation ISM and gas, i.e. H II regions, the Galactic Centre and Supernovae Remnants. IR emission due to fine-structure lines, molecular hydrogen, silicates, polycyclic aromatic hydrocarbons and dust are summarised, their diagnostic capabilities illustrated and their implications highlighted.

1. Introduction

Massive stars provide much of the radiative stellar energy of the Milky Way. Their copious amount of UV radiation has a big impact on the surroundings of the massive star. Indeed, their UV radiation dissociates molecules and dust in the interstellar medium (ISM) and ionises hydrogen, creating large H II regions. In addition, their powerful winds and supernova explosions provide most of the mechanical energy of the Galaxy which dominate the structure of the ISM. Furthermore, the nuclear reactions during their lifetime and death scene synthesis most of the intermediate mass elements and likely the r-process elements. Much of these nucleosynthetic products may condense in the form of small dust grains. Indeed, supernova may dominate the dust mass budget of the ISM. Because massive stars evolve so fast, they are generally associated with the remnants of their "cradle" and are heavily enshrouded in dust and gas. The gas and dust around these stars absorbs most of the stellar luminosity which is then re-emitted

---

in the infrared. Hence, due to the high degree of obscuration, massive stars can be best studied at wavelengths longer than 2 μm.

Offering unique combinations of wavelength coverage, sensitivity, and spatial and spectral resolutions in the infrared spectral region, ISO opened the infrared Universe. Its spectral coverage (from 2.3 – 200 μm) gives for the first time access to nearly all the atomic fine-structure and hydrogen recombination lines in the infrared range. In addition to the atomic lines, ISO revealed the shape and strength of the dust continuum and several emission features. This presented an unprecedented view of the luminous but dusty and obscured Universe, from the Galactic Centre to the most extincted regions of the Milky Way and other galaxies.

This chapter reviews the major achievements of ISO on massive stars. Sect. 2 summarises the results on H II regions, the Galactic Centre is discussed in Sect. 3. Subsequently, Sect. 4 highlights the ISO results on supernova remnants.

2. H II regions

The overall mid-IR (MIR) spectrum of H II regions is dominated by a dust continuum which rises strongly towards longer wavelengths (Fig.1). On top of this continuum, there are a multitude of fine-structure lines and hydrogen recombination lines. The continuum emission is dominated by strong emission features at 3.3, 6.2, 7.7, 8.6 and 11.2 μm, generally attributed to Polycyclic Aromatic Hydrocarbons (PAHs). In some case, broad absorption features due to simple molecules (H_2O, CO, CO_2) in an icy mantle and/or narrow emission or absorption lines due to gaseous molecules (H_2, H_2O, CO_2, OH, C_2H_2) are present.

2.1. The line spectrum

2.1.1. *The ionised gas*
H II regions are prime targets to derive the present-day elemental abundances of the ISM. They are bright and are characterised by a large number of emission lines. Optical studies of abundance gradients in the Galaxy, however, present the problem that many H II regions are highly obscured by dust lying close to the Galactic plane. The arrival of the Kuiper Airborne Observatory (e.g. Simpson et al., 1995; Afflerbach et al., 1997; Rudolph et al., 1997) and the Infrared Astronomical Satellite (e.g. Simpson and Rubin, 1990) permitted measurements of elemental abundances of embedded compact and ultra-compact H II regions, obscured at optical wavelengths but observable in the infrared, and gave
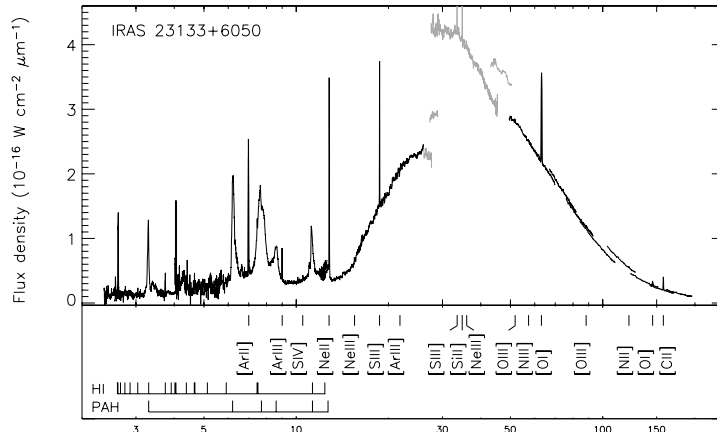
Figure 1. The ISO-SWS/LWS spectra of a typical H II region (Peeters et al. 2002b).

access for the first time to the central regions of the Galaxy. Regarding the determination of elemental abundances, the use of infrared fine-structure lines present clear advantages with respect to the optical lines (e.g. Rubin et al., 1988; Simpson et al., 1995): (1) they are attenuated much less due to the presence of dust; (2) they are practically insensitive to the precise temperature of the emitting gas since they are emitted from levels with very low excitation energies; and (3) the infrared range is the only wavelength regime to measure the dominant form of nitrogen in highly excited H II regions (N^{++}).

ISO provided a unique opportunity to measure the full spectral range from 2.3 to 196 μm of a large number of (ultra)compact H II regions with relatively good spectral and spatial resolution (e.g. Peeters et al., 2002b). Fig. 1 shows the combined SWS and LWS spectrum of a typical H II region. The spectrum is dominated by recombination lines of H and fine-structure lines of C, N, O, Ne, S, Ar and Si. The lines of [C II], [O I], and [Si II] are produced by ions with ionisation potentials lower than 13.6 eV and are thus expected to be mostly emitted in the PDR surrounding the H II region (see Sect. 2.1.2). Two lines are present for some of the ions (O^{++}, Ne^{++} and S^{++}), providing a handle on the electron density. Typically, [O III] 52, 88 μm densities towards Galactic H II regions range between $\sim$100 and 3000 cm^{-3} (cf. Martín-Hernández et al., 2002a). The use of the [S III] 18.7, 33.5 μm and [Ne III] 15.5, 36.0 μm line ratios requires careful aperture corrections. When such corrections are applied, the [S III] and [Ne III] densities agree well with the [O III] densities within the errors (cf. Martín-Hernández et al., 2003). N, Ne, Ar and S are observed in two different ioni-sation stages, which enormously alleviates the problem of applying
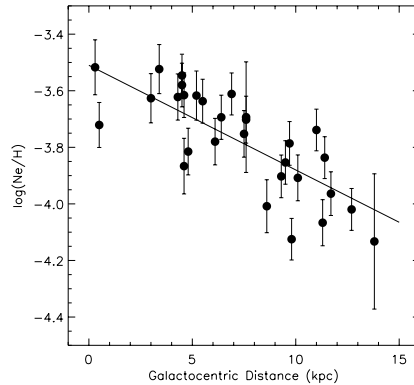
Figure 2. Neon abundance as a function of the distance to the Galactic Centre (cf. Martín-Hernández et al., 2002a).

ionisation correction factors (cf. Martín-Hernández et al., 2002a). The ISO observations of H II regions covered the Galactic plane from the centre to a Galactocentric distance of about 15 kpc, giving thus the possibility of investigating trends of relative and absolute elemental abundances across a large part of the Galactic disk. The gradients resulting from the full samples of Martín-Hernández et al. (2002a) and Giveon et al. (2002b) are $\Delta\log(Ne/H) = -0.039 \pm 0.007$, $\Delta\log(Ar/H) = -0.047 \pm 0.007$, $\Delta\log(S/H) = -0.023 \pm 0.014$ – re-computed by Giveon et al. (2002a) applying the same extinction and T_e corrections to both data sets – and $\Delta\log(N/O) = -0.056 \pm 0.009$ dex kpc^{-1}. Fig. 2 shows the neon abundance as a function of the distance from the Galactic Centre.

The direct observation of two different ionisation stages not only facilitates the determination of elemental abundances, but allows us to probe the ionisation structure of the H II regions and constrain the stellar energy distribution (SED) of the ionising stars. Line ratios such as [N III]/[N II] 57/122 μm, [Ne III]/[Ne II] 15.5/12.8 μm, [S IV]/[S III] 10.5/18.7 μm and [Ar III]/[Ar II] 9.0/7.0 μm probe the ionising stellar spectrum between 27.6 and 41 eV and depend on the shape of the SED and the nebular geometry (see e.g. Morisset et al., 2002, who present a detailed model of the well studied H II region G29.96–0.02 based on their infrared lines and Morisset et al., 2004, who compared predicted ionising spectra against ISO observations of Galactic H II regions). These line ratios are found to correlate well with each other for the large sample of H II regions observed by ISO (cf. Fig. 3) and to increase with Galactocentric distance (cf. Giveon et al., 2002b; Martín-Hernández et al. 2002a). The observed [Ne III]/[Ne II] and [S IV]/[S III] line ratios have been compared with diagnostic diagrams built from extensive
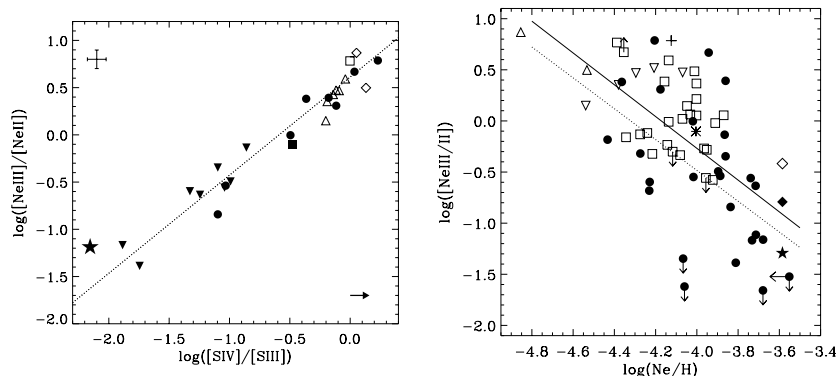
Figure 3. Left: Relation between the [S IV]/[S III] 10.5/18.7 μm and [Ne III]/[Ne II] 15.5/12.8 μm line ratios for a sample of H II regions (cf. Martín-Hernández et al., 2002b). Indicated by various symbols are Galactic regions at Galactocentric distance $R_{gal} < 7$ kpc (solid triangles), Galactic regions at $R_{gal} > 7$ kpc (solid circles), LMC regions (open triangles, except 30 Doradus, which is indicated by an open square) and SMC regions (open diamonds). The positions of Sgr A* (Lutz et al., 1996) and the Orion nebula (Simpson et al., 1998) are indicated by a solid star and a solid square, respectively. The dotted line is a least squares fit to the data. A typical error bar is given in the upper left corner. The arrow in the lower right corner indicates the correction due to an extinction $A_K = 2$ mag. Right: Relation between the [Ne III]/[Ne II] 15.5/12.8 μm line ratio and the Ne/H elemental abundance for a combined sample of H II regions (Martín-Hernández et al., 2003). Indicated by various symbols are Galactic H II regions (solid circles), Sgr A* (solid star), the Pistol and the Sickle (open and solid diamonds, respectively; Rodríguez-Fernández et al., 2001a), a sample of H II regions in M33 (open squares; Willner & Nelson-Patel, 2002), LMC H II regions (reverse open triangles, except 30 Doradus, which is plotted as a plus sign) and 2 regions in the SMC (open triangles).

photoionisation model grids computed for single-star H II regions using stellar atmosphere models from the WM-Basic code (Pauldrach et al., 2001) where the metallicities of both the star and the nebula have been taking into account (Morisset, 2004). This comparison finds no evidence of a gradient of the effective temperature of the ionising stars with the Galactocentric distance, attributing the observed increase of excitation with distance mainly to the effect of the metallicity gradient on the SED (see also Martín-Hernández et al., 2002b and Mokiem et al., 2004). The relation between the [Ne III]/[Ne II] line ratio and the Ne/H elemental abundance for a combined sample of Galactic and extra-galactic H II regions is shown in the left panel of Fig. 3. As it is evident from this figure, a clear correlation between excitation and metallicity exists, albeit with a large scatter.

Extended emission of highly-ionised species (fine-structure lines of N^+, N^{++}, O^{++} and S^{++}) have been detected by LWS and SWS (Mizu-

tani et al. 2002, Okada et al. 2003, Goicoechea et al. 2004). This reveals the presence of extended, highly ionised gas surrounding H II regions and probably ionised by the central O-star(s). The electron density has been derived from the [O III] 52 to 88 μm ratio, and values of a few 10 to a few 100 cm^{-3} have been found. This extended, ionised gas, denser than the galactic warm ionised medium would represent a new phase of the ISM as stressed by Mizutani et al. (2002).

Extragalactic studies of H II regions have been performed in the Magellanic Clouds (cf. Vermeij et al., 2002a; Vermeij & van der Hulst, 2002b) and M33 (Willner & Nelson-Patel, 2002). H II regions in the Magellanic Clouds are characterised by low metallicities and high excitation (see e.g. Fig. 3). Towards M33, the distribution of neon abundances as a function of Galactocentric radius is best described as a step gradient, with a slope of -0.15 dex from 0.7 to 4.0 kpc and -0.35 dex from 4.0 to 6.7 kpc.

2.1.2. *The photodissociation region*

Photodissociation Regions (PDRs) are regions where FUV ($6 < h\nu < 13.6$ eV) photons dissociate, ionise and heat neutral atomic/molecular gas surrounding H II regions (Tielens and Hollenbach 1985; Hollenbach and Tielens 1999). The gas reaches temperatures in the range 100-1000 K, much warmer than the dust (10-100 K), and radiates its energy in low energy atomic fine-structure lines, particularly the [O I] 63 μm, [C II] 157 μm, and [Si II] 34 μm lines, and in pure rotational molecular hydrogen lines (at wavelengths between 28 and 2 μm). In addition, the strong FUV flux pumps molecular hydrogen molecules into excited vibrational states and their cascade produces strong fluorescent rovibrational lines in the near-IR. The dust gives rise to a continuum at long wavelengths ($\lambda > 25$ μm). In addition, the IR spectrum of PDRs shows broad emission features at 3.3, 6.2, 7.7, 8.6, 11.2, and 12.7 μm due to fluorescent emission of FUV pumped Polycyclic Aromatic Hydrocarbon (PAHs) molecules (see Sect. 2.2). Here, we will focus on PDRs associated to H II regions; other PDRs are extensively discussed elsewhere in this book.

Because of their luke warm temperatures, PDRs were only 'discovered' when the IR window was opened by the Kuiper Airborne Observatory in the late 70ies and 80ies, but – because of limited sensitivities – these studies focused on the brightest objects in the sky (the Orion bar; Melnick et al., 1979; Storey et al., 1979, Russell et al., 1980, 1981). The increased sensitivities of the SWS and LWS and, in particular, their wide wavelength coverage allowed for the first time a systematic study of the properties of PDRs. Much of this data are however still resting in the archives. Except for the some of the ionic fine-structure lines and
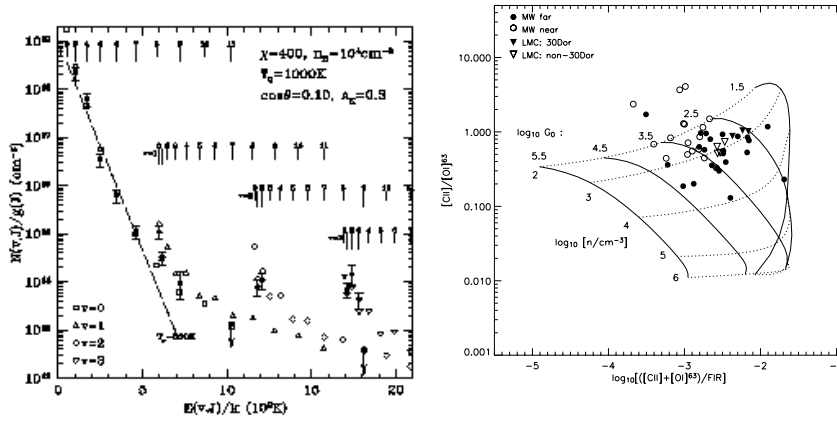
Figure 4. **Left :** The rotational diagram of molecular lines observed towards the bright rim cloud, S140 (Timmermann et al., 1996). Observed (filled symbols) and model calculated (open symbols) column densities (ratioed to the statistical weight of the level involved) are plotted as a function of the energy of the upper level. A Boltzmann distribution will show a straight line on this plot. The low lying pure rotational lines are consistent with gas at a kinetic temperature of 500 K. The higher excitation temperature of the vibrationally excited levels at high energies indicate the increased importance of FUV pumping for the populations of these levels. The models results are calculated for an incident FUV field of 400 times the average interstellar radiation field and a gas density of 10^4 cm^{-3}. A foreground extinction of 0.3 magnitudes in the K band has been adopted. T_o indicates the adopted peak temperature of the gas in the PDR. **Right :** A diagnostic diagram for PDRs based upon the intensity ratio of the [C II] 158 μm and the [O I] 63 μm lines and the overall cooling efficiency of the gas in the PDR. The lines present the results of detailed model calculations for a range in densities and incident FUV fields (Kaufman et al., 1999). The data are taken from LWS observations of a sample of H II regions (Peeters et al., 2002; 2005; Vermeij et al. 2002a).

the H I recombination lines, much of the IR emission characteristics of H II regions (Fig. 1), originate in the associated PDRs.

The SWS is particularly particularly suited for observations of the pure rotational lines of molecular hydrogen. These lines provide a direct handle on the physical properties of the emitting gas. Because of the small Einstein A's of the associated quadrupole transitions, the lowest levels of H_2 have very low critical densities and hence their populations are in local thermodynamic equilibrium for typical PDR conditions (Burton et al., 1992). A rotational diagram provides then directly the temperature and column density of the emitting gas. This is illustrated in Fig. 4, right panel, for the PDR associated with the blister H II region, S140 (Timmermann et al., 1996). The optically bright rim is produced by the ionisation of a dense clump in the molecular cloud, L1202/1204 by the nearby B0.5 star, HD 211880 (Blair et al., 1978; Evans et al., 1987). The SWS spectrum of this source shows pure rotational H_2 lines

up to $0 - 0$ $S(9)$. The column density and temperature derived from these observations are $N \simeq 10^{20}$ cm^{-2} and $T_{rot} = 500$ K (Timmermann et al., 1996). Similar studies of the pure rotational lines in the spectra of S106 and Cep A resulted in excitation temperatures of 500 and 700 K (van den Ancker et al., 2000; Wright et al., 1996).

In addition, SWS has observed several ro-vibrational lines in S140 belonging to the v =1–0, 2–1, and 3–2 series. These levels are populated by FUV pumping. Fig. 4, right panel, compares the observations with a detailed model for the collisional and FUV-pumping excitation of H$_2$ in this source (Timmermann et al., 1996). Good agreement is obtained for a density of 10^4 cm^{-3} in the PDR and an incident FUV flux of $\simeq$400 Habing. These values are consistent with estimates based upon pressure equilibrium across the ionisation front coupled with the ionised gas density in the associated bright rim and the properties of the illuminating star.

While this agreement between observations and models of H$_2$ excitation is very comforting (Fig. 4, right panel), PDR models have a problem in matching the observed kinetic temperatures and column densities derived from the low lying pure rotational lines. In particular, for such low FUV fields and densities as derived for S140, the calculated gas temperatures in the PDR are much lower than the observed 500 K (e.g. Draine & Bertoldi, 1999). This problem seems to be more general, although a detailed comparison of observations and models for regions spanning a wide range in physical properties is still wanting. Nevertheless, it seems that PDR models may be missing an essential part of the energetic coupling between the gas and the illuminating stellar FUV radiation field.

The far-IR atomic fine-structure lines provide important probes of the physical conditions in PDRs. However, at present, little has been done to harvest the data provided by the LWS. The [O I] 63 μm and [C II] 157 μm lines are the dominant coolants of PDRs (Tielens and Hollenbach 1985). Hence, the summed flux of these lines measures the total heating of PDR gas by the FUV radiation field. Comparison with the total incident FUV flux, as measured by the far-IR dust continuum provides a measure of the heating efficiency of PDRs. The levels involved in these two transitions have very different critical densities ($\sim 10^5$ and 3×10^3 cm^{-3}) and excitation energies (92 and 228 K). Not coincidentally, these values are precisely the range expected for gas in PDRs and, hence, the ratio of these lines has evolved to a major diagnostic of the properties of PDRs. This is illustrated in Fig. 4, right panel, where the results of PDR models for this line ratio are plotted against the calculated ratio of the cooling lines as a function of density and incident FUV field (Kaufman et al., 1999). Over much

of the relevant range of these observables, the model result segregate out well and hence this diagram is very useful for the analysis of the conditions in PDRs.

Observations towards a sample of H II regions are also shown in Fig. 4, left panel. The conditions in these regions span a range in density, $30\text{-}3 \times 10^3$ cm^{-3} and incident FUV fields, $3 \times 10^2 - 3 \times 10^4$ Habing. These values are within the range expected for PDRs associated with (evolved) compact H II regions. In addition, there seems to be a trend in the distribution of the observed points with location in the galaxy or, equivalently, metallicity. That is regions with lower metallicity seem to be characterised with a higher heating efficiency and lower [C II]/[O I] ratio than regions with higher metallicity. If the [O I] line is the dominant cooling line, a decrease in the metallicity is expected to result in a decreased [C II]/[O I]ratio (Tielens and Hollenbach 1985). However, the decrease in the heating rate with increasing metallicity is not expected. Further analysis of these types of observations is clearly warranted.

The fine-structure lines observed towards several individual high mass star forming regions have been analysed in detail. Analysis of the observations of W49N show that the PDR is illuminated by an intense FUV field ($G_o = 3 \times 10^5$). The density and temperature are, however, quite moderate ($n = 10^4$ cm^{-3}, $T = 130$K). Reflecting this high FUV field and low density, the observed heating efficiency is comparatively low, $\sim 10^{-4}$ (Vastel et al., 2001). Towards S106IR, a hot (200-500K) dense ($n > 3 \times 10^5$ cm^{-3}) gas component is present. Cooler gas is associated with the bulk of the emission of the molecular cloud and is characterised by 2 emission peaks which have densities of 10^5 cm^{-3} and are illuminated by a radiation field, G_0, ranging from 10^2 to $10^{3.5}$ (Schneider et al., 2003). The H II region S 125 is modelled self-consistently with a 2-dimensional geometrical blister model. In order to fit the spatial profile, a systematic increase of the gas temperature along the PDR boundary with decreasing distance from the ionising star is necessary, which is not readily understood within present-day PDR models (Aannestad & Emery, 2003). Despite the rich concentration of massive stars in the stellar cluster, Trumpler 14, in the Carina nebula, the physical conditions in the associated PDR are much less extreme than for Orion or M17 (Brooks et al., 2003). The data for the PDR in NGC 2024, on the other hand, are consistent with emission from dense ($n \simeq 10^6$ cm^{-3}), coolish ($T \simeq 100$ K) clumps (Giannini et al., 2000).

Finally, the lowest pure rotational $J = 1 - 0$ transition of the HD molecule at 112 μm was detected towards the Orion Bar using the LWS on ISO (Wright et al., 1999). The observations imply a total HD column density of $(3 \pm 0.8) \times 10^{17}$ cm^{-2} for adopted temperatures in the range 85–300 K. This corresponds to an elemental D/H abundance

ratio of $(2 \pm 0.6) \times 10^{-5}$, comparable to that derived from D I and H I ultraviolet absorption measurements in the solar neighbourhood.

2.2. PAHs and dust

Besides the well-known UIR bands at 3.3, 6.2, 7.6/7.8, 8.6, 11.2 and 12.7 μm, and very broad structures present underneath these bands, many discrete weaker bands and subcomponents can be found at 3.4, 3.5, 5.2, 5.7, 6.0, 6.6, 7.2–7.4, 8.2, 10.8, 11.0, 12.0, 13.2 and 14.5 μm. ISO extended the observable wavelength range and found there new feature at 16.4 μm and 17.4 μm as well as a weak, variable, emission plateau between 15 and 20 μm (Moutou et al., 2000; Van Kerckhoven et al., 2000; Van Kerckhoven, 2002). It should be emphasized that not all sources show all these emission features at the same time.

ISO also allowed, for the first time, a systematic analysis of the UIR bands in a wide variety of environments. It is now firmly established that the detailed characteristics (intensity, peak position, profile) of the UIR features vary from source to source and also spatially within extended sources (for a recent review, see Peeters et al., 2004b). ISO-SWS spectra indicated that the UIR band profiles and positions of all H II regions are equal to each other and to those observed in Reflection Nebulae (RNe), non-isolated Herbig AeBe stars and the ISM, while they are clearly distinct from those found around evolved stars and isolated Herbig AeBe stars (Fig. 5, Peeters et al. 2002a, van Diedenhoven et al. 2004). However, spatial variations within RNe (Bregman & Temi, 2004) and evolved stars (Kerr et al., 1999; Song et al., 2004; Miyata et al., 2004) are observed suggesting that in all sources profile variations occur on a small spatial scale. In addition, - in contrast to what the integrated spectra of sources might suggest - the profiles are not unique to certain object types. In contrast, their relative strength in H II regions varies both from source to source and within sources (Fig. 5). Integrated spectra of sources show variations in the relative strength of the CC modes (6–9 μm range) relative to the CH modes (at 3.3 and 11.2 μm), as is the 11.2/12.7 band ratio while the 3.3 μm feature correlates with the 11.2 μm feature and the 6.2 μm feature with the 7.7 μm feature (Fig 5, Roelfsema et al., 1996; Verstraete et al., 1996; Hony et al., 2001; Vermeij et al., 2002c). These variations are directly related to object type (Hony et al., 2001) and to the local environment (Fig 5, Verstraete et al., 1996; Vermeij et al., 2002c). Within extended sources, additional variations are found, nicely demonstrated by that of the 6.2/7.7 band ratio in S106 (Joblin et al., 2000). Within a single object, variations in G_0 are important in driving the UIR emission spectrum (Onaka, 2000; Bregman & Temi, 2004). However, the source to source
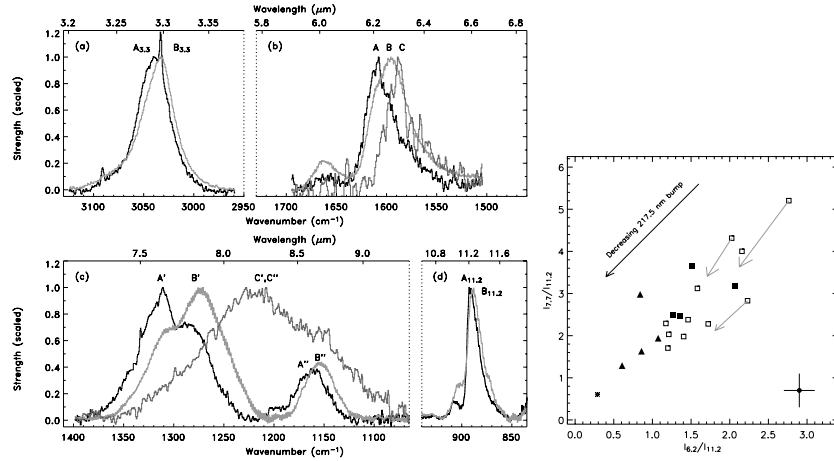
Figure 5. Left: Source to source variations for the 3–12 μm UIR bands. Profile A represent H II regions, Reflection Nebulae and the ISM, profile B isolated HAeBe stars and most PNe and profile C 2 post-AGB stars (Peeters et al. 2002a; van Diedenhoven et al. 2004). Right : PAH band strength ratios for H II regions. Galactic sources are shown as □, non-30 Dor sources as ■, 30 Dor pointings as ▲ and the SMC B1♯1 molecular cloud (Reach et al. 2000a) by an asterisk (Vermeij et al. 2002).

variation does not seem to follow G_0 (Verstraete et al., 2001; Hony et al., 2001; Peeters et al., 2002a; Vermeij et al., 2002c; van Diedenhoven et al., 2004; Peeters et al., 2004c).

The observed variations of the UIR bands provide direct clues to the physical and chemical properties of their carriers, the local physical conditions and/or the local history of the emitting population. These spectral variations have been attributed to a range of different physical or chemical characteristics of the carriers, including charge state, anharmonicity, different subcomponents with variable strength, family of related species with varying composition, substituted/complexed PAHs, isotope variations, clustering, molecular structure, molecular composition etc. (Verstraete et al., 1996; Joblin et al., 2000; Verstraete et al., 2001; Hony et al., 2001; Pech et al., 2002; Peeters et al., 2002a; Wada et al., 2003; Song et al., 2004; Bregman & Temi, 2004; Hudgins & Allamandola, 2004; van Diedenhoven et al., 2004). In particular, the variations in the 11.2/6.2 and 3.3/6.2 μm ratios likely reflect variations in the average ionization state of the emitting PAHs. In contrast, the variations in the peak position of the 6.2 μm band point towards variations in the molecular structure of the emitting species perhaps related to the incorporation of N into the ring structure of the PAHs.

Since the UIR bands are omnipresent, they serve as important probes of the different emission zones. For example, the presence and strength of the UIR bands are generally thought to trace star formation and

so they are used as qualitative and quantitative diagnostics of the physical processes powering Galactic nuclei (see this issue). In addition, deuterated PAHs are tentatively detected at 4.4 and 4.65 μm at high abundances in the Orion Bar and M17 (Peeters et al., 2004a). If born out, they can serve as probes of PAH D/H ratio in various regions.

Several studies were devoted to the spatial distribution of the different emission components (Cesarsky et al., 1996; Verstraete et al., 1996; Pilbratt et al., 1998; Créte et al., 1999; Klein et al., 1999; Zavagno & Ducci, 2001; Urquhart et al., 2003; Verma et al., 2003). It is overwhelmingly clear that the UIR bands peak in the PDR, though closer to the ionized star with respect to H_2, while the strong dust continuum peaks towards the H II region. Inside the H II region, where UIR bands are weak or absent, remains a broad underlying emission band which is attributed to very small grains (VSG, Cesarsky et al., 1996; Jones et al. 1999). The spatial distribution of the UIR bands is also displaced from that of the ERE emission in Sh 152 (Darbon et al., 2000), similar to the Red Rectangle (Kerr et al., 1999). It is clear that the carrier of the UIR bands is not also responsible for the ERE. Moreover, because the ERE emission can sometimes be traced to inside the ionized gas and recalling that the PAHs do not survive in the H II region, the carrier of the ERE is unlikely to be molecular in origin.

The dust/UIR band emission has been modeled for several sources. Créte et al. (1999) modeled M17 using a 2-component model composed of PAHs as the carrier of the UIR bands and VSG responsible for the "warm" continuum and a 2-component model composed of coal dust emission and big grain emission. In the frame of the coal dust model, the observations required nano-sized, transiently heated particles. The IR emission in the M17-SW H II region and Orion is modeled with a mixture of amorphous carbons, silicates and possibly crystalline silicates (see below, Jones et al., 1999; Cesarsky et al. 1996). PAHs seem to be depleted inside the H II region consistent with their destruction in the intense radiation field of M17 and Orion (Jones et al., 1999; Cesarsky et al., 2000; Créte et al., 1999). Modelling of the FIR emission of Sh 125 also indicates the dust to be severely depleted in the H II region while normal dust/gas ratio is observed in the PDR, but with a major fraction in the form of VSG (Aannestad & Emery, 2001).

ISO also increased the number of H II regions showing silicate in emission (Cesarsky et al., 2000; Peeters et al., 2002b; Peeters, 2002) and detected several new dust features :

1) A very strong, broad 8.6 μm band is detected towards the M17-SW H II region and 3 compact H II regions, clearly distinct from the "classical" 8.6 μm PAH band and originating inside the H II regions (Roelfsema et al., 1996; Cesarsky et al., 1996; Verstraete et al., 1996;

Peeters et al., 2002a; Peeters et al., 2004d). Detailed analysis reveals the feature having a profile peaking at 8.9 μm with a FWHM ~ 1 μm and likely not being related to PAH emission (Peeters et al., 2004d).

2) A broad 22 μm feature is detected in the M17-SW H II region (Jones et al., 1999), the Carina Nebula and two starburst galaxies (Chan & Onaka, 2000). The feature shape is similar to that of the 22 μm band observed in Cassiopeia A indicating that supernovae are probably the dominant production sources (Chan & Onaka, 2000).

3) Several (possible) detections of crystalline silicates associated with H II regions are reported, i.e. (i) emission at 34 μm in the M17 H II region attributed to Mg-rich crystalline olivine (Jones et al., 1999); (ii) emission bands at 9.6 μm in θ^2 Ori A and at $\sim$ 15-20 μm, $\sim$ 20-28 μm and longward of 32 μm in the Orion H II region attributed to crystalline Mg-rich silicate fosterite (Cesarsky et al., 2000). The latter emission bands are however a combination of instrumental effects and the PAH 15-20 μm plateau (Kemper et al., in preparation); (iii) a band at 65 μm in the Carina Nebula and Sh 171 attributed to diopside (Ca-bearing crystalline silicate - Onaka & Okada, 2003). An upper-limit for the crystallinity of the silicates in the ISM is derived being a few % (Jones et al., 1999), less than 5% (Li & Draine, 2001) and less than 0.4% (Kemper et al., 2004).

4) To end, a broad emission feature is found at 100 μm in the Carina Nebula and Sh 171, possibly due to carbon onion grains (Onaka & Okada, 2003). A similar broad feature around 90 μm is reported in evolved stars and a low mass protostar, attributed to calcite, a Ca-bearing carbonate mineral (Ceccarelli et al., 2002; Kemper et al., 2002).

3. The Galactic Centre

The 500 central pc of the Galaxy (hereafter Galactic center, GC) are an extended source of emission at all wavelengths from radio to γ-rays (see Mezger et al., 1996 for a review). The non-thermal radio emission as well as γ and X-rays observations show the presence of a very hot plasma ($10^7 - 10^8$ K) and a recent episode of nucleosynthesis ($\sim 10^6$ yr ago) that suggest an event of violent star formation in the recent past. On the other hand, the cold medium in the GC is mainly known by radio observations of the molecular gas. In between these hot and cold phases, there is a warm (few hundred K) neutral medium and a thermally ionized medium. ISO has made important contributions to our understanding of the heating of the warm neutral gas and the properties of the ionized gas in the GC.

Before ISO, the ionized gas has been mainly studied by radio continuum and hydrogen radio recombination lines observations. They showed an extended diffuse ionized gas component and a number of discrete H II regions, most of them associated with the Sgr A, B,... complexes. Only the most prominent H II regions (Sgr A) and ionized nebulae (the Sickle) had been observed in infrared fine-structure lines. ISO observations of fine-structure lines allowed studying the properties of the ionized gas and the ionizing radiation over the whole GC region. In the vicinity of Sgr A*, where the ionizing source is the central stellar cluster, Lutz et al. (1996) derived an effective temperature of the ionizing radiation of $\sim$ 35000 K and Rodríguez-Fernández et al. (2001a) derived a similar effective temperature in the Radio Arc region. They also showed unambiguously that the Quintuplet and the Arches clusters ionize the Sickle nebula and the thermal filaments that seem to connect Sgr A to the Radio Arc. Indeed, the combined effects of both clusters ionize a region of more that 40×40 pc^2. Their photo-ionization model simulations showed that, in order to explain the long-range effects of the radiation, the ISM that surrounds the clusters must be highly inhomogeneous. A similar scenario has been invoked by Goicoechea et al. (2004) to explain the extended ionized gas component in the Sgr B molecular complex. Indeed, the whole GC region is permeated by relatively hot ($\sim$ 35000 K) but diluted ionizing radiation field (Rodríguez-Fernández & Martín-Pintado, 2004).

The line ratios ([Ne III]/[Ne II] 15.5/12.8 μm, [N III]/[N II] 57/122 μm ...) measured in the GC are similar to those found in low excitation starburst galaxies as M 83 or IC 342 but somewhat lower than those measured in other starburst galaxies as NGC 3256 or NGC 4945. However, the low ratios do not imply intrinsic differences in the star formation activity as a lower upper mass cutoff of the initial mass function. On the contrary, they are probably due to starburst of short duration that produce hot massive stars but whose age quickly softens the radiation (Thornley et al., 2000). The ISO observations of the GC are consistent with a burst of star formation less than 7 Myr ago.

On the other hand, in the GC there is a widespread neutral gas component with temperatures of $\sim$ 200 K and without associated warm dust. Before ISO, this warm neutral gas had only been studied by radio observations of symmetric top molecules like NH$_3$. How this gas is heated has been a long-standing problem. Radiative heating mechanisms are usually ruled out due to the apparent lack of continuum sources and the discrepancy of gas and dust temperatures. ISO was perfectly suited to study the heating of this gas. First, Rodríguez-Fernández et al. (2001b) have measured for the first time the total amount of warm gas in the GC clouds by observing H$_2$ pure rotational
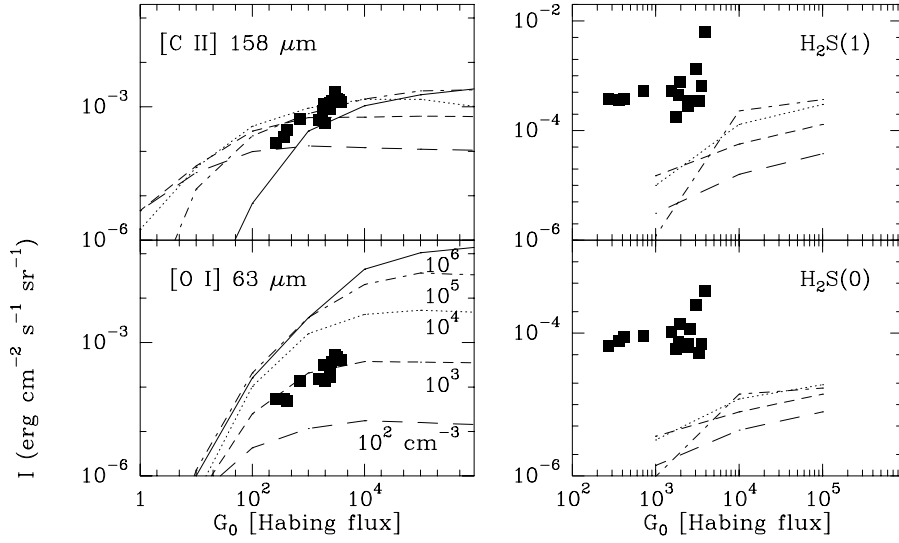
Figure 6. Intensities of two fine-structure lines and two H_2 pure-rotational lines versus the far-ultraviolet incident flux derived for the sources observed by Rodríguez-Fernández et al. (2004b). For comparison, the PDR model predictions (Tielens & Hollenbach, 1985) for different densities are also shown.

lines. These lines trace gas with temperature from 150 K to 500 K. The column density of gas with a temperature of 150 K is a few 10^{22} cm^{-2} and, on average, it is around 30% of the total gas column density. Second, ISO has observed the main coolants of the neutral gas (the [C II]158 and [O I]63 μm lines) with temperatures of a few hundred K and the full continuum spectrum of the dust emission around the maximum. The dust emission can be characterized by two temperature components, one with a temperature of $\sim$ 15 K and a warmer one with a temperature that varies from source to source from $\sim$ 25 to $\sim$ 45 K (Lis et al., 2001; Rodríguez-Fernández et al., 2004; Goicoechea et al. 2004). A detailed comparison of the lines and continuum emission with shocks and PDR models show that the fine structure lines and the H_2 emission from excited levels arise in a PDR with a far-ultraviolet incident radiation field 10^3 times higher than the average local interstellar radiation field and a density of 10^3 cm^{-3}(Rodríguez-Fernández et al. 2004). The warm dust emission and the fine-structure lines probably arise in PDRs located in the interface between the ionized gas discussed above and the cold molecular gas. Rodríguez-Fernández et al. (2004) also showed that an important fraction ($\sim$ 50%) of the [C II]158 and [Si II]35 μm can arise from the diffuse ionized gas instead of the PDR itself. Regarding the warm H_2, only 10-20 % of the total column density of gas with temperature of 150 K can be accounted for in the widespread PDRs
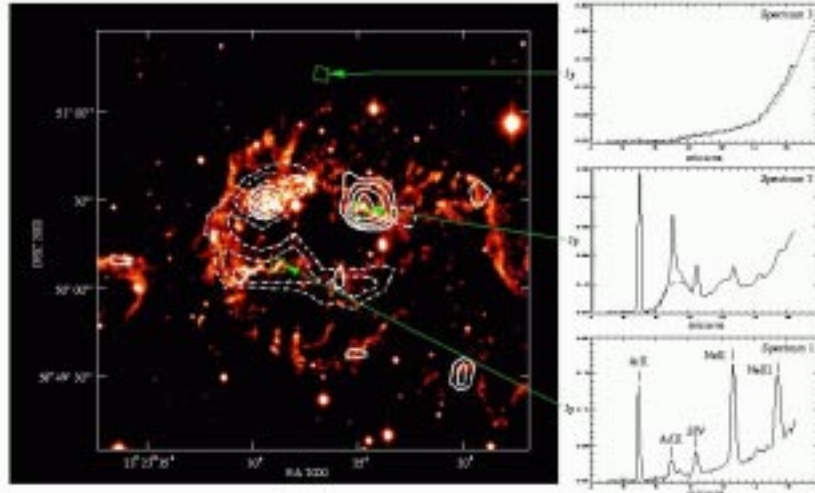
Figure 7. Contour maps of the [Ne II] 12.8 μm line emission (dotted contours) and of the 9.5 μm silicate dust emission (full contours) plotted onto an optical image of the Cassiopeia-A supernova remnant. Examples of the variety seen in the MIR spectra are shown on the right [Taken from Douvion et al. 1999].

scenario. The most likely heating mechanism for the bulk of the warm neutral gas is the dissipation of magneto-hydrodynamic turbulence or low velocity shocks.

Spectroscopic imaging/mapping will be useful to investigate the interplay between the different ISM phases in the GC. This could be done with the IRS instrument onboard the Spitzer Space Telescope. In addition, SOFIA and Herschel will be able to map the ionized and the warm neutral gas with high spectral resolution, which is needed due to the crowded velocity fields in the GC region.

4. Supernova Remnants (SNRs)

As the prototype of O-rich young SNR, Cassiopeia A is well-studied by ISO (Lagage et al., 1996; Tuffs et al., 1997; Arendt et al., 1999; Douvion et al., 1999; Douvion et al., 2001b). Several fine-structure lines are observed at high velocity with [OIV] being the most prominent (e.g. Fig.7). However, no iron emission is observed (Arendt et al., 1999). These fine-structure lines are spatially correlated with the Fast Moving Knots (FMKs) known to be made of nuclear burning products from the progenitor star. While fainter diffuse dust emission is present, the brightest continuum emission is spatially correlated with the fine-

structure lines indicating that dust has freshly condensed in the FMKs. The high dust temperature derived is consistent with emission from collisionally heated dust in the post-shock region of FMKs. A new 22 μm feature is found and identified with Mg protosilicates (Arendt et al., 1999). However, Mg protosilicates give rise to a 10 μm feature quite different from the observed one (Douvion et al., 2001b). These authors fitted a 6–30 μm spectrum of Cas A with SiO_2, $MgSiO_3$, Al_2O_3. In addition to dust continuum emission, silicate emission is present at several positions within Cas A (Fig.7). The presence of silicate and the presence of neon is anti correlated in many knots while argon and sulfur are present in most of the neon knots (Fig.7), suggesting a different degree of mixing occurred (Douvion et al., 1999). These results also indicate an incomplete condensation of silicate elements. If born out for other core collapse SNe, these SN can no longer be considered the dominant source of silicates (Douvion et al., 1999). Similar conclusion was reached by Tuffs et al. (1997) based upon the derived dust mass being less than a few hundredths of a solar mass.

In contrast to Cas A, the dust emission in the Kepler and Tycho SNR is spatially correlated with Hα emission and therefore attributed to shocked circumstellar (CS) material and CS or interstellar (IS) material respectively and not to SN condensates. Instead of dust signatures, the Crab SNR is dominated by synchrotron radiation with a spectral index of -0.3 to -0.65. Fine-structure lines of [Ne II] and [Ar II] are observed for the Kepler SNR and of [Ne II], [Ne III], [Ne V], [Ar II], [Ar III], [S IV], [Ni II] for the Crab SNR. The [Ne III] emission in the Crab SNR shows the same filamentary structure as seen in optical lines, known to be composed predominately of SN ejecta (Douvion et al., 2001a).

The IR spectrum of RCW103, a young and fast SNR, is dominated by prominent lines from low-excitation species allowing estimates of electron density, temperature and abundances. The ionic lines are consistent with post-shock emission. The absence of significant emission from the pre-shock region suggests that shock models may overestimate the importance of the precursor. All - but one - abundances are solar and hence the emitting gas is ISM material in which the dust grains have been destroyed by the shock front (Oliva et al., 1999b).

The interaction of SNR with molecular clouds has been extensively studied with ISO. The IR spectra of the SNRs 3C 391, W44 and W28 exhibit fine-structure line emission, dust emission along the line of sight and shocked dust emission shortwards of 100 μm (Reach & Rho, 1996, 2000; Reach et al., 2002). In addition, shock-excited FIR emission of H_2O, CO and OH emission is detected in 3C 391 (Reach & Rho, 1998). These IR observations provide evidence for multiple pre- and post-shock conditions which are found to be spatially separated. Indeed,

ISOCAM-CVF observations clearly resolves the ionic emission from the molecular emission tracing moderate-density to high density regions in 3C 391. Abundance analysis reveal partial dust destruction consistent with theoretical models of grain destruction. Similar, spectral variations are observed spatially within IC443 (Cesarsky et al., 1999; Oliva et al., 1999a; Rho et al., 2001). The north-easthern filamentary structure is dominated by prominent [Ne II], [Fe II], [S III], [O IV] and [O I] line emission while the southern clumpy region is dominated by H_2 emission indicating different types of shock occuring in different conditions. Both regions can alone account for virtually all the observed IRAS flux in the 12 and 25 μm bands – likely due to the limited ISO field-of-view and limited IRAS spatial resolution. Despite this, the unusually blue IRAS colors of IC443 reflect line (molecular and/or atomic) contamination instead of a large population of small grains.

The late emission of SN1987A probes directly the elemental abundances deep in the stellar ejecta and as such constrains models of SN explosion and the explosive nucleosynthesis. Particularly important for this are the ^{56}Ni, ^{57}Ni and ^{44}Ti masses. The former two are known, the latter is more uncertain and can be derived from the [Fe I]24.05 μm and [Fe II]25.99 μm fine-structure lines. These lines are however not detected in the ISO spectra of SN1987A indicating – based upon time dependent models – an upper limit of 1.1 10^{-4} $M_{\odot}$ (Lundqvist et al. 1999; 2001). The central region around the SN position is resolved in the MIR and consistent with collisionally heated grains in the shocked CS gas around SN1987A (Fischera et al., 2002a). The MIR spectrum can be modeled by a dust mixture of silicate-iron or silicate-graphite or pure graphite grains and indicates a low dust-to-gas ratio (Fischera et al., 2002a).

Hence, observations of ionic lines allow to diagnose the physical conditions of the medium in which the SNR blast wave is propagating, the shock kinematics, the elemental abundances and hence also dust destruction. ISO provided evidence that dust can form in supernovae and dust can be (partially) destroyed in supernovae.

References

Aannestad, P.A., Emery, R.J. Modeling FIR emission from the H II region S125 *Astronomy and Astrophysics*, 376:1040-1053, 2001.

Aannestad, P.A., Emery, R.J. Modeling FIR line emission from the H II region Sh 125. *Astronomy and Astrophysics*, 406:155–164, 2003

Afflerbach, A., Churchwell, E., Werner, M. W. Galactic abundance gradients from IR fine-structure lines in compact H II regions. *Astrophysical Journal*, 478:190, 1997.

Arendt, R.G., Dwek, E., Moseley, S.H. Newly synthesized elements and pristine dust in the Cas A supernova remnant. *Astrophysical Journal*, 521:234–245, 1999

Blair, G. N.; Evans, N. J., II; vanden Bout, P. A.; Peters, W. L., III The energetics of molecular clouds. II - The S140 molecular cloud. *Astrophysical Journal*, 219:896-913, 1978

Bregman, J. & Temi, P. Wavelength Shifts of the 7.7 Micron Emission Band in Reflection Nebulae *Astrophysical Journal*, 2004, submitted.

Brooks, K.J., Cox, P., Schneider, N., Storey, J.W.V., Poglitsch, A., Geis, N., Bronfman, L. The Trumpler 14 PDR in the Carina Nebula. *Astronomy and Astrophysics*, 412:751–765, 2003

Burton, Michael G.; Hollenbach, D. J.; Tielens, A. G. G. M. *Astrophysical Journal*, 399:563-572, 1992

Ceccarelli, C.; Caux, E.; Tielens, A. G. G. M.; Kemper, F.; Waters, L. B. F. M.; Phillips, T. Discovery of calcite in the solar type protostar NGC 1333-IRAS 4 *Astronomy and Astrophysics*, 395:L29-L33, 2002

Cesarsky, D., Lequex, J., Abergel, A., Perault, M., Palazzi, E., Madden, S., Tran, D. IR spectrophotometry of M17 with ISOCAM. *Astronomy and Astrophysics*, 315:L309-L312, 1996.

Cesarsky, D., Cox, P., Pineau des Forets, G., van Dishoeck, E.F., Boulanger, F., Wright, C.M. ISOCAM spectro-imaging of the H_2 rotational lines in the supernova remnant IC443. *Astronomy and Astrophysics*, 348:945-949, 1999.

Cesarsky, D., Jones, A.P., Lequex, J., Verstraete, L. Silicate emission in Orion. *Astronomy and Astrophysics*, 358:708-716, 2000.

Chan, K.-W., Onaka, T. A broad 22 μm emission fature in the carina nebula H II region. *Astrophysical Journal*, 533:L33-L36, 2000.

Créte, E., Giard, M., Joblin, C., Vauglin, I., Léger, A., Rouan, D. Grain populations in the M17 south-west star forming complex. *Astronomy and Astrophysics*, 352:277-286, 1999.

Darbon, S., Zavagno, A., Perrin, J.-M., Savine, C., Ducci, V., Sivan, J.-P. Extended red emission and unidentified infrared bands in the galactic compact H II region Sh 152. *Astronomy and Astrophysics*, 364:723-731, 2000.

Draine, B.T., Bertoldi, F. Heating the gas in phtodissociation fronts. The universe as seen by ISO, ESA-SP 427, p553, 1999.

Douvion, T., Lagage, P.O., Cesarsky, C.J. Element mixing in the Cassiopeia A supernova. *Astronomy and Astrophysics*, 352:L111–L115, 1999

Douvion, T., Lagage, P.O., Cesarsky, C.J., Dwek, E. Dust in the Tycho, Kepler and Crab supernova remnants. *Astronomy and Astrophysics*, 373:281–291, 2001a

Douvion, T., Lagage, P.O., Pantin, E. Cassiopeia A dust composition and heating. *Astronomy and Astrophysics*, 369:589–593, 2001b

Evans, Neal J., II; Kutner, Marc L.; Mundy, Lee G. VLA observations of H2CO in absorption against the cosmic background radiation - Clumps in the S140 molecular cloud. *Astrophysical Journal*, 323:145-153, 1987

Fischera, Jg., Tuffs, R.J., Volk, H.J. IR emission towards SN1987A 11 years after outburst : Measurments with ISOCAM. *Astronomy and Astrophysics*, 386:517-530, 2002a

Fischera, Jg., Tuffs, R.J., Volk, H.J. IR emission towards SN1987A 11 years after outburst : Properties of the circumstellar dust. *Astronomy and Astrophysics*, 395:189-200, 2002b

Giannini, T., Nisini, B., Lorenzetti, D., Di Giorgio, A.M., Spinoglio, L. et al. Looking at the PDR in NGC2024 through FIR line emission. *Astronomy and Astrophysics*, 358:310–320, 2000

Giveon, U., Sternberg, A., Lutz, D., Feuchtgruber, H. and Pauldrach, A. W. A. The excitation and metallicity of Galactic H II regions from ISO/SWS observations of MIR fine-structure lines. *Astrophysical Journal*, 566:880–897, 2002b.

Giveon, U., Morisset, C. and Sternberg, A. The ISO Galactic metallicity gradient revisited. *Astronomy and Astrophysics*, 392:501–503, 2002a

Goicoechea, J. R., Rodríguez-Fernández, N. J. and Cernicharo,J. The FIR Spectrum of the Sagittarius B2 Region: Extended Molecular Absorption, Photodissociation, and Photoionization. *Astrophysical Journal*, 600:1214-233, 2004.

Hollenbach, D. J.; Tielens, A. G. G. M. Photodissociation regions in the interstellar medium of galaxies. *Reviews of Modern Physics*, 71, 173-230, 1999

Hony, S., Van Kerckhoven, C., Peeters, E., Tielens, A. G. G. M., Hudgins, D. M., Allamandola, L. J. The CH out-of-plane bending modes of PAH molecules in astrophysical environments. *Astronomy and Astrophysics*, 370:1030–1043, 2001.

Hudgins, D. M., Allamandola, L. J. Aromatic Hydrocarbons and IR Astrophysics : The state of the PAH model and a posssible tracer of Nitrogen in C-rich dust. *Astrophysics of Dust Astronomical Society of the Pacific*, p665, 2004.

Joblin, C., Abergel, A., Bregman, J., d'Hendecourt, L., Heras, A. M. et al. Spectroscopic diversity of the UIR bands as revealed by ISO: Towards a molecular carrier identification. ISO beyond the peaks ESA-SP 466, 2000.

Jones, A.P., Frey, V., Verstraete, L., Cox, P., Demyk, K. The IR emission from dust in the M17-SW H II region : partially crystalline silicates in the ISM? The universe as seen by ISO, ESA-SP 427, p679, 1999.

Kaufman, M.J.; Wolfire, M.G.; Hollenbach, D.J.; Luhman, M.L. Far-Infrared and Submillimeter Emission from Galactic and Extragalactic Photodissociation Regions. *Astrophysical Journal*, 527:795-813, 1999

Kemper, F.; Molster, F. J.; Jger, C.; Waters, L. B. F. M. The mineral composition and spatial distribution of the dust ejecta of NGC 6302. *Astronomy and Astrophysics*, 394:679-690, 2002

Kemper, F.; Vriend, W. J.; Tielens, A. G. G. M. The Absence of Crystalline Silicates in the Diffuse ISM. *Astronomy and Astrophysics*, 609:826-837, 2004

Kerr, T.H., Hurst, M.E., Miles, J.R., Sarre, P.R. Observations of the 3.3 μm UIR band in the Red Rectangle: relation to unidentified optical emission. *Mon. Not. R. Astron. Soc.*, 303:446-454, 1999.

Klein, R., Henning, T., Cesarsky, D. The molcular cloud core M7-north : New ISOCAM observations. *Astronomy & Astrophysics*, 343: L53-56, 1999.

Li, A., Draine, B.T. On Ultrasmall Silicate Grains in the Diffuse Interstellar Medium. *Astrophysical Journal*, 550:L213-L217, 2001

Lagage, P.O., Claret, A., Ballet, J., Boulanger, F., Cesarsky, C.J. et al. Dust formation in the Cassiopeia A supernova. *Astronomy and Astrophysics*, 315, L274–L276, 1996

Lis, D.C., Serabyn, E., Zylka R., Li Y. Quiescient giant molecular cloud cores in the Galactic center. *Astrophysical Journal*, 550: 761-777, 2001.

Lundqvist, P., Sollerman, J., Kozma, C., Larsson, B., Spyromilio, J. et al. ISO SWS/LWS observations of SN1987A. *Astronomy and Astrophysics*, 347, 500–507, 1999

Lundqvist, P., Kozma, C., Sollerman, J., Fransson, C. ISO/SWS observations of SN1987A II. A refined upper limit on the mass of ^{44}Ti in the ejecta of SN1987A. *Astronomy and Astrophysics*, 374:629–637, 2001

Lutz, D. Feuchtgruber, H. Genzel, R. Kunze, D. Rigopoulou, D. et al. SWS observations of the Galactic center. *Astronomy & Astrophysics*, 315: L269-L272, 1996.

Martín-Hernández, N. L., van der Hulst, J. M., and Tielens, A. G. G. M. A radio continuum and IR study of Galactic H II regions. *Astronomy and Astrophysics*, 407:957–985, 2003.

Martín-Hernández, N. L., Vermeij, R., Tielens, A. G. G. M., van der Hulst, J. M., and Peeters, E. The stellar content, metallicity and ionization structure of H II regions. *Astronomy and Astrophysics*, 389:286–294, 2002b.

Martín-Hernández, N. L., Peeters, E., Morisset, C., Tielens, A. G. G. M., Cox, P. et al. ISO spectroscopy of compact H II regions in the Galaxy. II Ionization and elemental abundances. *Astronomy and Astrophysics*, 381:606–627, 2002a.

Mathis, J. S. and Rosa, M. R. Ionization correction factors and compositions of H II regions. *Astronomy and Astrophysics*, 245:625–634, 1991.

Melnick, G.; Gull, G. E.; Harwit, M. Observations of the 63 μm forbidden OI emission line in the Orion and Omega Nebulae. *Astrophysical Journal*, 227:L29-L33, 1979.

Mezger, P. G., Duschl, W. J. and Zylka, R. The Galactic Center: a laboratory for AGN? *Astronomy & Astrophysics Review*, 7: 289-388, 1996.

Mizutani, M., Onaka, T., Shibai, H. Detection of highly-ionized diffuse gas in the Galactic plane. *Astronomy & Astrophysics*, 382, 610, 2002

Miyata, T., Kataza, H., Okamoto, Y. K., Onaka, T., Sako, S. et al. Sub-arcsecond imaging and spectroscopic observations of the Red Rectangle in the N-band. *Astronomy and Astrophysics*, 415:179–187, 2004.

Mokiem, M. R., Martín-Hernández, N. L., Lenorzer, A., de Koter, A. and Tielens, A. G. G. M. Metallicity and the spectral energy distribution and spectral types of dwarf O-stars. *Astronomy and Astrophysics*, 419:319–334, 2004.

Morisset, C., Schaerer, D., Martín-Hernández, N. L., Peeters, E., Damour, F. et al. A photoionization model of the compact H II region G29.96–0.02. *Astronomy and Astrophysics*, 386:558–570, 2002.

Morisset, C. O star effective temperatures and H II region ionization parameter gradients in the Galaxy. *Astrophysical Journal*, 601:858–863, 2004.

Morisset, C., Schaerer, D., Bouret, J.-C., and Martins, F. MIR observations of Galactic H II regions: Constraining ionizing spectra of massive stars and the nature of the observed excitation sequences. *Astrophysical Journal*, 415:577–594, 2004.

Moutou, C., Verstraete, L., L'eger, A., Sellgren, K., Schmidt, W. New PAH mode at 16.4 μm. *Astronomy and Astrophysics*, 354:L17–L20, 2000.

Oliva, E., Moorwood, A.F.M., Drapatz, S., Lutz, D., Sturm, E. IR spectroscopy of young supernova remnants heavily interacting with the interstellar medium I. Ionized species in RCW103. *Astronomy and Astrophysics*, 343:943–952, 1999b

Oliva, E., Lutz, D., Drapatz, S., Moorwood, A.F.M. ISO/SWS spectroscopy of IC443 and the origin of the IRAS 12 and 25 μm emission from radiative supernova remnants. *Astronomy and Astrophysics*, 341:L75–L78, 1999a

Okada, Y., Onaka, T., Shibai, H., Doi, Y. Mid- to Far-IR spectroscopy of Sh 171. *Astronomy and Astrophysics*, 412:199–212, 2003

Onaka, T. Interstellar Dust: What do Space Observations Tell Us? *Advances in Space Research*, 25:2167–2176, 2000

Onaka, T., Okada, Y. Detection of FIR features in star-forming regions. *Astrophysical Journal*, 585:872–877, 2003.

Pauldrach, A. W. A., Hoffmann, T. L. and Lennon, M. Radiation-driven winds of hot luminous stars. XIII. A description of NLTE line blocking and blanketing towards realistic models for expanding atmospheres. *Astronomy and Astrophysics*, 375:161–195, 2001.

Pech, C., Joblin, C., Boissel, P. The profiles of the aromatic infrared bands explained with molecular carriers. *Astronomy and Astrophysics*, 388:639–651, 2002.

Peeters, E., Allamandola, L. J., Bauschlicher, C. W., Hudgins, D. M., Sandford, S. A., Tielens, A. G. G. M. Deuterated Interstellar Polycyclic Aromatic Hydrocarbons. *Astrophysical Journal*, 604:252–257, 2004a.

Peeters, E., Allamandola, L. J., Hudgins, D. M., Hony, S., Tielens, A. G. G. M. The UIR features after ISO. *Astrophysics of Dust Astronomical Society of the Pacific*, p141, 2004b.

Peeters, E., Spoon, H. W. W., Tielens, A. G. G. M. PAHs as a tracer of star formation? *Astrophysical Journal*, 613, 2004c.

Peeters, E., Tielens, A. G. G. M., Boogert, A. C. A., Hayward, T. L., Allamandola, L. J. A new prominent 8.9 μm emission feature in H II regions. *Astrophysical Journal*, 2004d, submitted.

Peeters, E. PAHs and dust in regions of massive star formation. *PhD thesis, University of Groningen, The Netherlands*, 2002.

Peeters, E., Hony, S., Van Kerckhoven, C., Tielens, A. G. G. M., Hudgins, D. M., Allamandola, L. J., Bauschlicher, C. W. The rich 6 to 9 μm spectrum of interstellar PAHs. *Astronomy and Astrophysics*, 390:1089–1113, 2002a.

Peeters, E., Martín-Hernández, N. L., Damour, F., Cox, P., Roelfsema, P. R. et al. ISO spectroscopy of compact H II regions in the Galaxy. I The catalogue. *Astronomy and Astrophysics*, 381:571–605, 2002b.

Pilbratt, G.L., Altieri, B., Blommaert, J.A.D.L., Fridlund, C.V., Tauber, J.A., Kessler, M.F. ISOCAM images of the 'elephant trunks' in M16. *Astronomy and Astrophysics*, 333:L9–L12, 1998.

Reach, W.T., Rho, J. Shockingly bright [OI] 63 μm lines from the supernova remnants W44 and 3C391. *Astronomy and Astrophysics*, 315, L277–L280, 1996

Reach, W.T., Rho, J. Detection of FIR water vapor, hydroxyl and carbon monoxide emissions from the supernova remnant 3C 391. *Astrophysical Journal*, 507, L93–L97, 1998

Reach, W.T., Boulanger, F.; Contursi, A.; Lequeux, J. Detection of mid-IR aromatic hydrocarbon emission features from the Small Magellanic Cloud. *Astronomy and Astrophysics*, 361:895-900, 2000a

Reach, W.T., Tho, J. IR spectroscopy of molecular supernova remnants. *Astrophysical Journal*, 544:843–858, 2000b

Reach, W.T., Tho, J., Jarrett, T.H., Lagage, P.-O. Molecular and ionic shocks in the supernova remnant 3C391. *Astrophysical Journal*, 564:302–316, 2002

Rho, J., Jarrett, T.H., Cutri, R.M., Reach, W.T. NIR imaging and [O I] spectroscopy of IC443 using 2MASS and ISO. *Astrophysical Journal*, 547:885-898, 2001

Rodríguez-Fernández, N. J., Martín-Pintado, J. Fuente, A. de Vicente, P. Wilson, T. L. and Hüttemeister Warm H_2 in the Galactic center region. *Astronomy & Astrophysics*, 377: 631–643, 2001b.

Rodríguez-Fernández, N. J.,Martín-Pintado, J. and de Vicente, P. Large scale ionization of the Radio Arc region by the Quintuplet and the Arches clusters. *Astronomy & Astrophysics*, 377: 631–643, 2001a.

Rodríguez-Fernández, N. J. and Martín-Pintado ISO observations of the Galactic center ISM: ionized gas. *Astronomy & Astrophysics*, in press, 2004.

Rodríguez-Fernández, N. J.,Martín-Pintado, J., Fuente, A. and Wilson, T. L. ISO observations of the Galactic center ISM: neutral gas and dust. *Astronomy & Astrophysics*, in press, 2004.

Roelfsema, P. R., Cox, P., Tielens, A. G. G. M., Allamandola, L. J., Baluteau, J.-P. et al. SWS observations of IR emission features towards compact HII regions. *Astronomy and Astrophysics*, 315, L289–L292, 1996

Rubin, R. H., Simpson, J. P., Erickson, E. F. and Haas, M. R. Determination of N/O from FIR line observations of Galactic H II regions. *Astrophysical Journal*, 327:377–388, 1988.

Rudolph, A. L., Simpson, J. P., Haas, M. R., Erickson, E. F. and Fich, M. FIR Abundance Measurements in the Outer Galaxy. *Astrophysical Journal*, 489:94, 1997.

Russell, R. W.; Melnick, G.; Smyers, S. D.; Kurtz, N. T.; Gosnell, T. R.; Harwit, M.; Werner, M. W. Giant forbidden C II halos around H II regions. *Astrophysical Journal*, 250:L35-L38, 1981.

Russell, R. W.; Melnick, G.; Gull, G. E.; Harwit, M. Detection of the 157 micron/1910 GHz CII emission line from the interstellar gas complexes NGC 2024 and M42. *Astrophysical Journal*, 240:L99-L103, 1980.

Schneider, N., Simon, R., Kramer, C., Kraemer, K., Stutzki, J., Mookerjea, B. A moltuwavelength study of the S106 regiona II. Characteristics of the PDR. *Astronomy and Astrophysics*, 406:915–935, 2003

Simpson, J. P. and Rubin, R. H. IRAS low-resolution spectral observations of H II regions. *Astrophysical Journal*, 354:165–183, 1990.

Simpson, J. P., Colgan, S. W. J., Rubin, R. H., Erickson, E. F. and Haas, M. R. FIR lines from H II regions: Abundance variations in the galaxy. *Astrophysical Journal*, 444:721–738, 1995.

Simpson, J. P., Witteborn, F. C., Price, S. D. and Cohen, M. Midcourse Space Experiment Spectra of the Orion Nebula and the Implications for Abundances in the Interstellar Medium. *Astrophysical Journal*, 508:268–274, 1998.

Song, I.-O.; Kerr, T. H.; McCombie, J.; Sarre, P. J. Evolution of the 3.3 μm emission feature in the Red Rectangle. *Mon. Not. R. Astron. Soc*, 346:L1–L5, 2004

Storey, J. W. V.; Watson, D. M.; Townes, C. H. Observations of far-infrared fine structure lines - Forbidden O III 88.35 microns and forbidden O I 63.2 microns *Astrophysical Journal*, 233:109-118, 1979.

Tielens, A.G.M.M. and Hollenbach, D. Photodissociation regions. I. The basic model. *Astrophysical Journal*, 291:722–754, 1985

Timmermann, R., Bertoldi, F., Wright, C.M., Drapatz, S., Draine, B.T., Haser, L., Sternberg, A. H_2 IR line emission from S140 : a warm PDR. *Astronomy and Astrophysics*, 315:L281–L284, 1996

Thornley, M. D., Schreiber, N. M. F. Lutz, D.,Genzel, R., Spoon, H. W. W.,Kunze, D. and Sternberg, A. Massive Star Formation and Evolution in Starburst Galaxies: MIR Spectroscopy with ISO/SWS. *Astrophysical Journal*, 539: 641–657, 2000.

Tuffs, R.J., Drury, L.O.'C., Fischera, J., Heinrichsen, I., Rasmussens, I., Russell, S., Wolk, H.J. Spectrophotometry of dust and gas in Cassiopeia A and the Cygnus Loop. *First ISO Workshop on Analytical Spectroscopy, ESA-SP419*, 177, 1997.

Urquhart, J.S., White, G.J., Pilbratt, G.L., Fridlund, C.V.M. ISOCAM-CVF imaging of M16. *Astronomy and Astrophysics*, 409:193-203, 2003.

van den Ancker, M.E., Tielens, A.G.G.M., Wesselius, P.R. ISO spectroscopy of the young bipolar neulae S106IR and Cep A East. *Astronomy and Astrophysics*, 358:1035–1048, 2000

van Diedenhoven, B., Peeters, E., Van Kerckhoven, C., Hony, S., Hudgins, D. M., Allamandola, L. J., Tielens, A. G. G. M. The profiles of the 3 to 12 μm PAH features. *Astrophysical Journal*, 611:928-939 , 2004.

Van Kerckhoven, C., Hony, S., Peeters, E., Tielens, A. G. G. M., Allamandola, L. J. et al. The C-C-C bending modes of PAHs: a new emission plateau from 15 to 20 μm *Astronomy and Astrophysics*, 357:1013–1019, 2000.

Van Kerckhoven, C. PAHs and diamonds arounc YSOs. *PhD thesis, Catholic University of Leuven, Belgium*, 2002.

Vastel, C., Spaans, M. Ceccarelli, C., Tielens, A.G.G.M., Caux, E. The physical conditions in the PDR of W49 N. *Astronomy and Astrophysics*, 376:1064–1072, 2001

Verma, R.P., Ghosh, S.K., Mookerjea, B., Rengarajan, T.N. Far and mid-IR observations of two ultracompact H II regions and one compact CO clump. *Astronomy and Astrophysics*, 398:589-605, 2003.

Vermeij, R., Damour, F., van der Hulst, J. M., and Baluteau, J.-. P. The physical structure of Magellanic Cloud H II regions. I. Dataset. *Astronomy and Astrophysics*, 390:649–665, 2002a.

Vermeij, R. and van der Hulst, J. M. The physical structure of Magellanic Cloud H II regions. II. Elemental abundances. *Astronomy and Astrophysics*, 391:1081–1095, 2002b.

Vermeij, R., Peeters, E., Tielens, A. G. G. M., van der Hulst, J. M. The PAH emission spectra of Large Magellanic Cloud H II regions. *Astronomy and Astrophysics*, 382:1042–1051, 2002c.

Verstraete, L., Puget, F. L., Falgarone, E., Drapatz, S., Wright, C. M., Timmermann, R. SWS spectroscopy of small grain features across the M17-Southwest photodissociation front. *Astronomy and Astrophysics*, 315:L337–L340, 1996.

Verstraete, L., Pech, C., Moutou, C., Sellgren, K., Wright, C. M., Giard, M., L'eger, A., Timmermann, R., Drapatz, S. The Aromatic IR Bands as seen by ISO-SWS: Probing the PAH model. *Astronomy and Astrophysics*, 372:981– 997, 2001.

Wada, S., Onaka, T., Yamamura, I., Murata, Y., Tokunaga, A. T. ^{13}C isotope effects on infrared bands of quenched carbonaceous composite (QCC). *Astronomy and Astrophysics*, 407:551–562, 2003.

Willner, S. P. and Nelson-Patel, K. Neon Abundances in the H II Regions of M33. *Astrophysical Journal*, 568:679–688, 2002.

Wright, C.W., Drapatz, S., Timmermann, R., van der Werf, P.P., Katterloher, R., de Graauw, Th. Molecular hydrogen observations of Cepheus A West *Astronomy and Astrophysics*, 315, L301-L304, 1996

Wright, C.W., van Dishoeck, E.F., Cox, P., Sidher, S.D., Kessler, M.F. ISO-LWS Detection of the 112 Micron HD J = 1 –> 0 Line toward the Orion Bar *Astrophysical Journal*, 515, L29-L33, 1999

Zavagno, A., Ducci, V. ISOCAM 3-12 μm imaging of fice galactic compact H II regions. *Astronomy and Astrophysics*, 371:312-327, 2001.